



# Characterisation of induced discontinuities in the Boom Clay around the underground excavations (URF, Mol, Belgium)

J. Mertens<sup>a,\*</sup>, W. Bastiaens<sup>b</sup>, B. Dehandschutter<sup>c</sup>

<sup>a</sup> ONDRAF/NIRAS Belgian Agency for Radioactive Waste and Enriched Fissile Materials, Avenue des Arts 14, BE-1210 Brussels, Belgium

<sup>b</sup> EIG EURIDICE, Boeretang 200, BE-2400 Mol, Belgium

<sup>c</sup> Structural geology and tectonics group, KULeuven, Redingenstraat 16, BE-3000 Leuven, Belgium

Received 15 March 2003; received in revised form 17 July 2003; accepted 7 September 2003

Available online 2 April 2004

## Abstract

Excavation works were carried out in Boom Clay to extend the underground research facility in Mol (Belgium) located at a depth of 223 m below the surface. The attempt to characterise the extent of the Excavation Damaged Zone, or EDZ, around the second shaft, using seismic measurements and cored borings, was successful, as proven by observations during further excavation works in the investigated area. No evidence for the occurrence of natural discontinuities was found. Using an industrial technique, an 84-m-long gallery was excavated in the Boom Clay. These excavation works induced a symmetrical pattern of discontinuities and clearly limited the EDZ extent.

© 2004 Elsevier B.V. All rights reserved.

*Keywords:* Fractures; Clay; Excavation Damaged Zone (EDZ); Shear planes; Seismic campaign; Cores

## 1. Introduction

The Boom Clay is a marine Oligocene deposit of several tens of meter thickness, which is of considerable stratigraphic and geotechnical significance in North Belgium (Fig. 1) (Vandenberghe, 1978, SAFIR II, 2001). Some characteristic properties are given in Table 1. The formation is currently under study as a host formation for the storage of high level and long-lived waste. These studies have been commissioned by the Belgian Agency for Radioactive Waste and Enriched Fissile Materials (ONDRAF/NIRAS). In

Mol, where the clay is located at depths between 185 and 287 m below surface, an underground research facility (HADES-URF) is situated at a depth of 223 m below surface (Fig. 2). During the 1980s, a first shaft and two galleries were constructed (URL and Test Drift). In 1999, a second shaft was excavated, 157 m away from the first one. Near the bottom, two Starting Chambers were constructed. One directing southward and one directing northward, towards the Test Drift. Previous to the final construction of the Connecting Gallery, which took place in 2002, a Mounting Chamber had to be constructed in order to be able to install the Tunnel Boring Machine (TBM).

During excavation of the Starting Chambers, large shear planes were detected, one of them leading to a major rock fall in the southern Starting Chamber. The

\* Corresponding author. Tel.: +32-2-212-10-03; fax: +32-2-218-51-65.

E-mail address: [mertens.dehul@pandora.be](mailto:mertens.dehul@pandora.be) (J. Mertens).

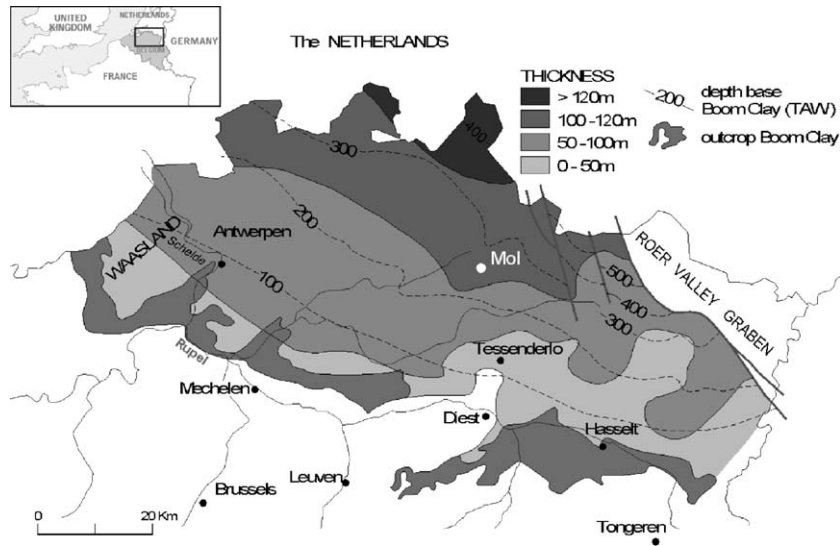


Fig. 1. Extension of the Boom Clay formation in the North of Belgium. The location of the HADES-URF in Mol is also indicated (after SAFIR II). The formation is gently dipping ( $\pm 1^\circ$ ) towards the North North–East.

shape of the extruded clay block suggested that there might be a circular pattern of shear planes around the second shaft. Before constructing the Mounting Chamber, a reconnaissance campaign, consisting of a borehole seismic campaign and two cored borings, revealed the extent of the Excavation Damaged Zone (EDZ) of the shaft and the Starting Chamber.

During manual excavation of the Mounting Chamber, fractures were observed, measured and characterised. The results of the reconnaissance campaign were compared with the observations made during excavation.

During excavation of the Connecting Gallery, using an industrial technique (see Bastiaens and Demarche, 2003, and further in this report), a characteristic pattern of discontinuities was encountered. Two cored borings, drilled after the full excavation of the Connecting

Table 1  
Characteristic properties of the Boom Clay

Bulk density (sat.)	1.9–2.1 t/m <sup>3</sup>
Water content	19–24%
Total porosity	36–40%
UCS	2.2–2.8 MPa
Young's modulus	200–400 MPa
Poisson's ratio	0.4
Cohesion	0.396 MPa
Internal friction	11°

Gallery, gave additional information about the extent of the EDZ.

In this paper, the observations and conclusions from the reconnaissance campaign are compared with the observations from the excavation of the Mounting Chamber. Conclusions on the origin of the fractures are formulated.

The observations of the fracture pattern during the construction of the Connecting Gallery is also presented and discussed below.

## 2. Reconnaissance campaign of the Mounting Chamber

Fig. 3 gives a plan view of the second shaft and the northern Starting Chamber, showing the location of four horizontal boreholes. Two of them, 2000–4 and 2000–5, were used for the seismic campaign. The other two, 2000–11 and 2001–2, were cored.

### 2.1. Seismic campaign

An interval velocity and cross-hole seismic campaign was performed in the two parallel boreholes 2000–4 and 2000–5 (see Fig. 3) by BGR (Hannover).

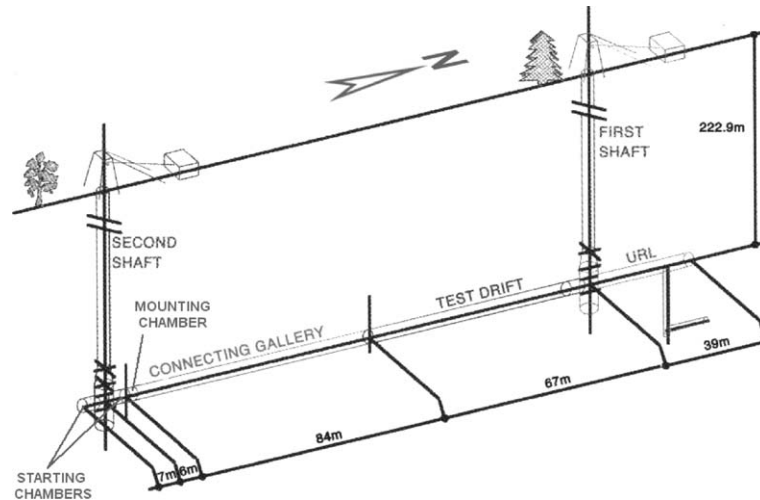


Fig. 2. Overview of the HADES-URF. During the 1980s, a first shaft and two galleries were constructed (URL and Test Drift). A second shaft was excavated in 1999, 157 m away from the first one. Near the bottom, two Starting Chambers were constructed, one directing south and one directing north, towards the Test Drift. Previous to the final construction of the Connecting Gallery, which took place in 2002, a Mounting Chamber had to be constructed, in order to be able to install the Tunnel Boring Machine (TBM).

The two boreholes were located symmetrically around the centre of the Starting Chamber, about 3.6 m away from each other. A mini-sonic probe was used to perform the measurements.

Fig. 4 shows the main results from the campaign. It appears that the rock mass is damaged with a lot of small-scale disturbances up to approximately 2 m (2.8 m in 2000–4 and 1 m in 2000–5). The region between 2 and 5 m shows less small-scale disturbances. It can be noticed that this zone presents a gradual increase of the P-wave velocity to an average level of 1900 m/s. An explanation for the phenomenon of the cross-hole P-wave velocity increase might be the increasing stress around the borehole with increasing distance from the second shaft and/or a decrease in the amount or the influence of fractures.

From their measurements, BGR concluded that there are indications that the EDZ extends to approximately 5 m into the clay body. A remarkable differentiation between the depth ranges 0.3–2 m and 2–5 m was noticed.

Further away from the shaft, between 8.5 m (9.2 m in 2000–04 and 7.4 m in 2000–05) and 13.5 m (14 m in 2000–04 and 13 m in 2000–05), where the interval velocity measurements had to be suspended, very strong velocity variations were observed, in connection with a high damping of amplitudes. The difference

between the single-hole and cross-hole velocities in the deeper part of the borehole can be found in the borehole damage. The borehole walls were highly disturbed (see Section 2.2), giving rise to a significant distortion of the single-hole measurements. The cross-hole measurements were performed 3 weeks after the casing and grouting of the borehole. It is very likely that convergence and the effect of grouting reduced the distortion of the velocities, caused by the disturbed borehole, for the cross-hole measurements.

## 2.2. Two cored borings

Two horizontal cored borings were performed.

Looking at Fig. 5, showing a plan view of the strike of all discontinuities encountered, it can be concluded that all but two discontinuities, located in 2001–2, have a strike perpendicular to the borehole axis. All discontinuities show striations, indicating a shear origin. The Striations appearing on the two out-of-line discontinuities are, however, more outspoken than the ones appearing perpendicular on the borehole. Dips are both directed towards the Mounting Chamber and away from it.

The strikes from the two out-of-line discontinuities are approximately tangential to circles around the second shaft. Both discontinuities are dipping towards

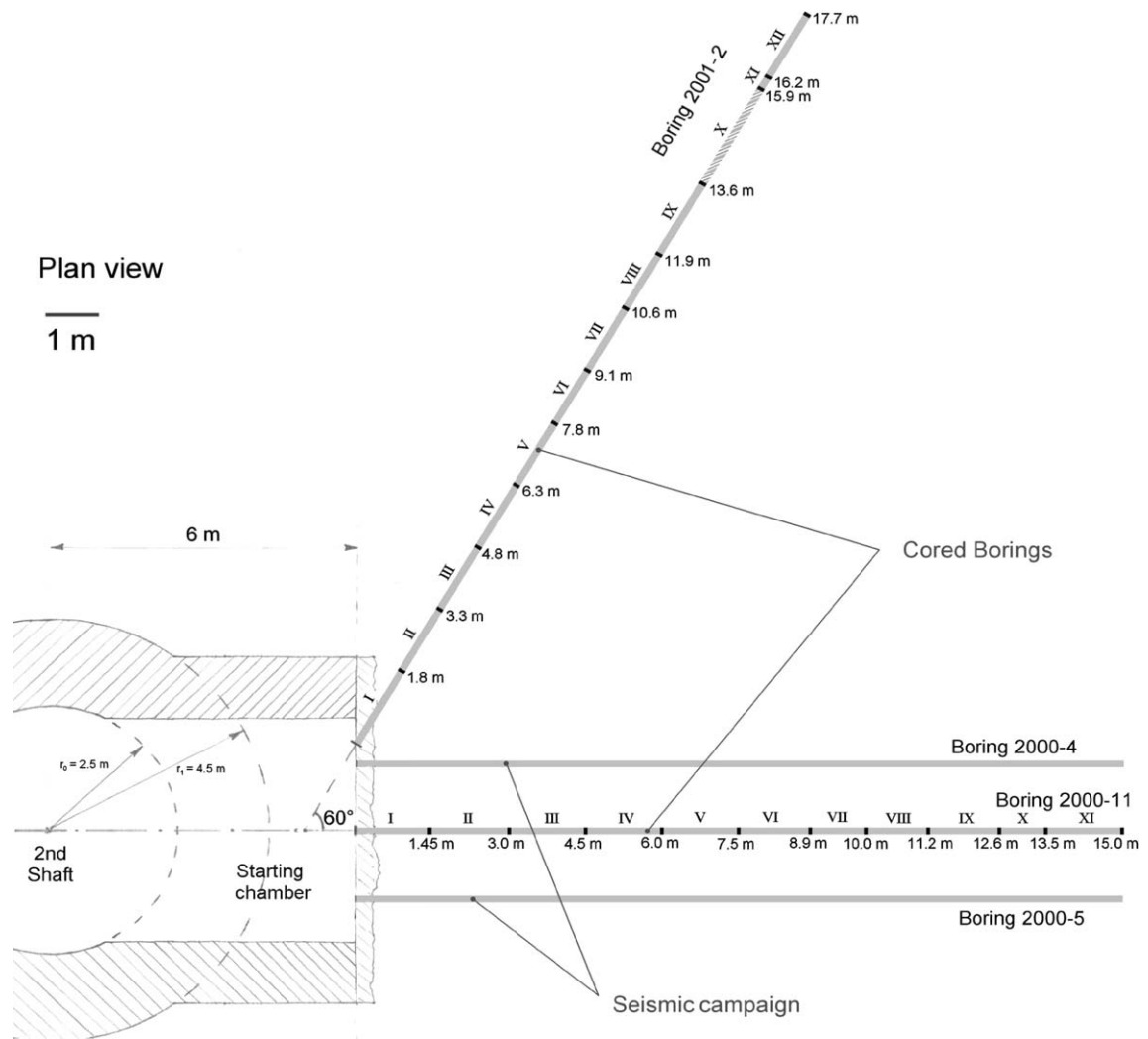


Fig. 3. Plan view of the second shaft at the depth of the northern Starting Chamber. The location of the boreholes used for seismic measurements (2000–4 and 2000–5) and the cored borings (2000–11 and 2001–2) are indicated.

the centre of the second shaft. Dips are  $34^\circ$  and  $38^\circ$ . The second one is located at a distance of more than 5 m from the Starting Chamber. This also seems to suggest that the idea of a pattern of circular-shaped large slip planes, dipping towards the centre of the second shaft is a valid one.

All other discontinuities from 2001–2 are perpendicular to the borehole axis, suggesting a drilling related origin.

In boring 2000–11, the distinction between both groups (drilling-related and others) could unfortunately

not be outlined, due to its direction. The fact that the striations of some shear planes in the first meters of the borehole are far more pronounced than others appearing near the end of the borehole or even show two striation directions (Fig. 5a) and that all discontinuities from 0 to 7 m in this borehole are dipping towards the centre of the second shaft, while further away both dip directions occur, might suggest that here too, the EDZ extends up to 7 m, although the data is too limited in this case to draw any significant conclusion.

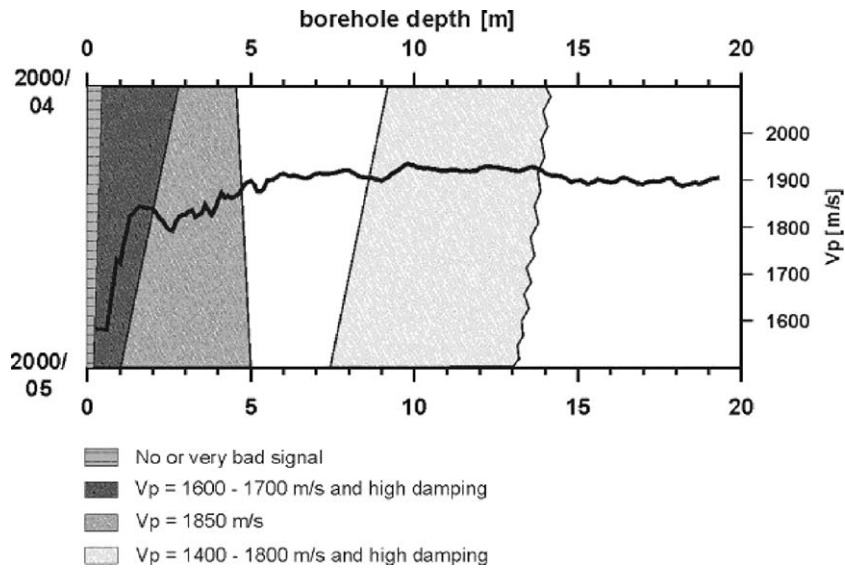


Fig. 4. Results from the seismic campaign by BGR. The curve shows the result of the cross-hole seismic measurements. The shaded surfaces are the correlations between both single-hole measurements. According to BGR, there are indications that the EDZ extends up to 5 m into the clay body.

In Fig. 5b, part of the last core taken from borehole 2001–2 is pictured. One can notice the intense fracturing due to the drilling process. A high concentration of these fractures, most of them appearing in pairs creating the form of bills of birds (Fig. 5c) appeared in the last cores of both drillings. Dips varied between  $40^\circ$  and  $60^\circ$ . It is clear, taking into account the strike of the discontinuities, that they are formed due to a relaxation of the clay in the direction of the bore axis. The fact that they do not appear in the first meters, or at least show a much lesser intensity there, can easily be explained by the allowance of a large convergence of the clay after the excavation of the second shaft and the Starting Chamber. The clay mass experienced relaxation, and the stresses are low in the first meters.

Another drilling effect, noticed when entering the borehole with a camera was that in the deeper part of the boreholes (7–15 m) pieces of clay, as indicated in Fig. 6, were expelled from the sidewalls of the borehole. These pieces were often recovered in the core tubes. The form of the borehole in this zone was very irregular. On the contrary, in the first meters of the borehole, the walls appeared to be rather intact. Again, this can be explained by relaxation of the clay in the first meters.

### 3. Excavation of the Mounting Chamber

During manual excavation of the Mounting Chamber, observations of discontinuities were systematically reported and, where possible, measured.

The encountered discontinuities can roughly be classified into four characteristic groups.

- Large shear planes ( $>3 \text{ m}^2$ )
- Small shear planes ( $<1 \text{ m}^2$ )
- Large tension fissures ( $>2 \text{ m}^2$ )
- Small tension fissures ( $<1 \text{ m}^2$ )

Shear planes with surfaces areas roughly between 1 and  $3 \text{ m}^2$  were not observed, nor tension fissures with surfaces ranging from 1 to  $2 \text{ m}^2$ .

It could clearly be outlined that small shear planes were created during the excavation of the Mounting Chamber itself, and small tension planes were created by this excavation and by local dehydration of the clay near the Starting Chamber due to unusual long (in the order of months) exposure to air.

In this paper, only the large shear planes and large tension planes will be considered.

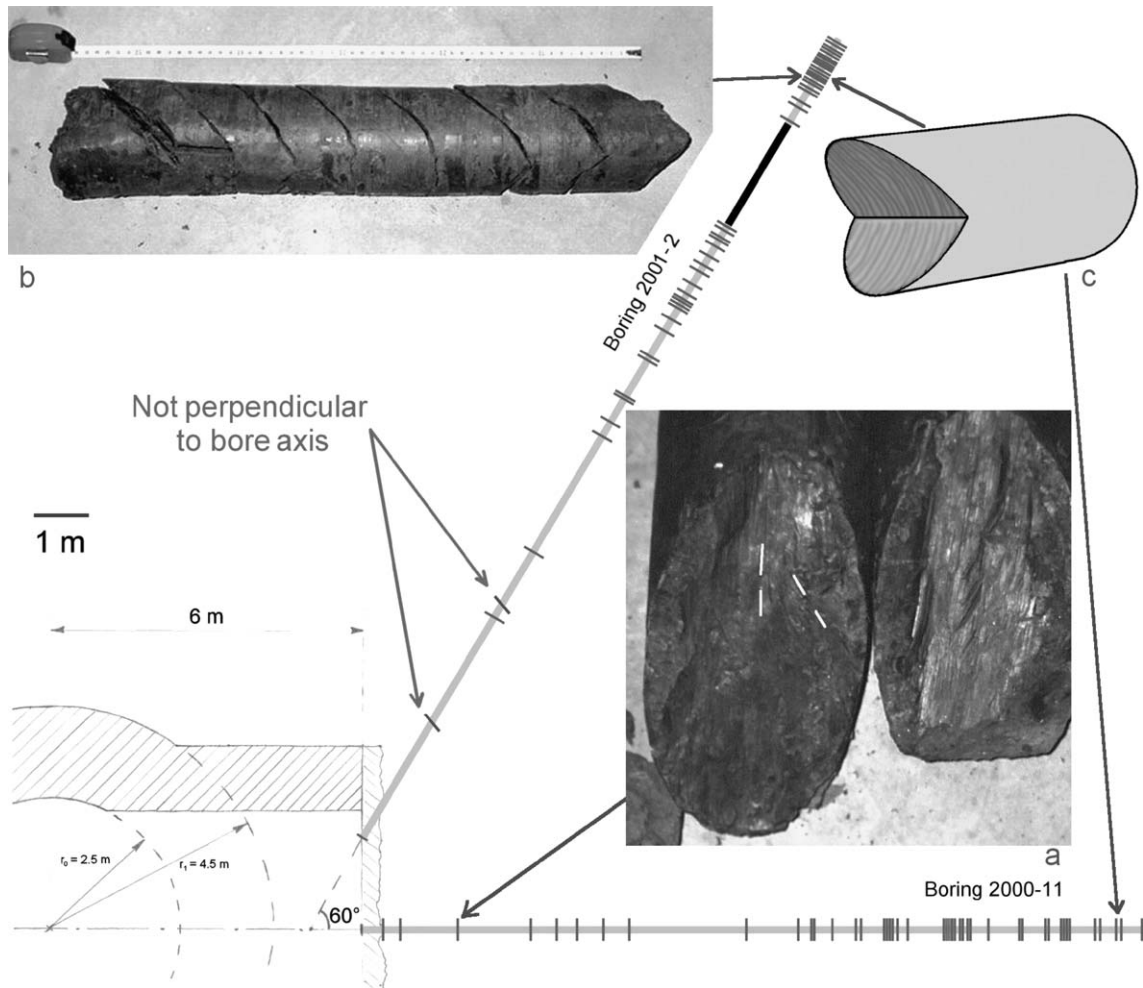


Fig. 5. Plan view of encountered discontinuities in the cored borings. In (a), a fracture containing striations in two directions is pictured. In (b), a picture from the highly fractured core near the end of the borehole is shown. In (c), the typical form of conjugated fractures in the cores near the end of the borehole is drawn. Unfortunately, core X in borehole 2001–2 was lost due to pyrite obstruction in front of the core-mouth.

### 3.1. Large shear planes

The most dominant discontinuities observed in the front are large ( $>3 \text{ m}^2$ ) slickensided shear planes, containing clear striations (Fig. 7). The planes are dipping towards the centre of the second shaft. They are more or less parallel and have an average spacing of around 70 cm. Their strike is  $\pm$  EW on an average. The dip ranges between  $30^\circ$  and  $70^\circ$ , due to the fact that most of the shear planes were curved in such a way that their dip increased with increasing distance from the shaft.

Some of the shear planes are curved in such a way that their dip becomes steeper with increasing distance from the centre of the shaft.

Striations are orientated on an average in the dip direction.

Especially in the first 1.5 m of excavation, the cross-section between these planes and the front always appears in the form of a bow (Fig. 8).

This supports the hypothesis that these planes are roughly circular around the second shaft (Fig. 9). The planes are continuous over the whole front width, and

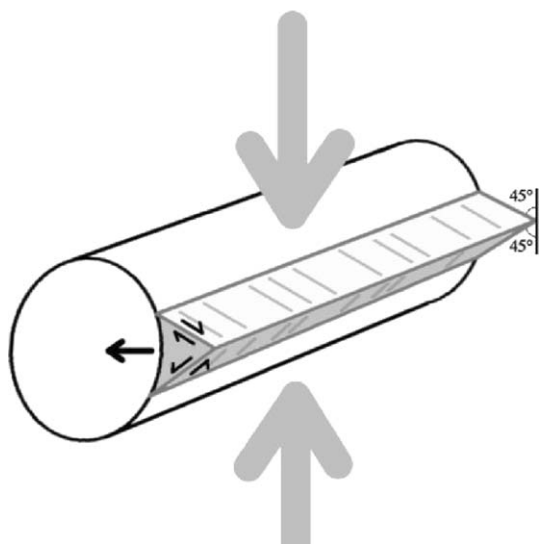


Fig. 6. Drawing of the expelled clay pieces along the borehole. These pieces were often recovered in the cores. They are clearly borehole breakouts which took place after the drilling process.

a lot of them extend further around a large part of the second shaft.

The fractures are open. Pyrite oxidation was present on the surfaces till 2 m of depth. Fractures show an aperture up to 3 cm before excavation. This is illustrated by the anchor resin, used for the installation

of some safety anchors before the excavation, which entered the open fractures and hardened out as a mould between the two fracture planes.

The observed shear planes are not always planar. Sometimes, a surface was undulating or splitted into several other shear planes.

Two different directions of striations are regularly observed.

In Fig. 10, a vertical cross-section through the middle of the Mounting Chamber was reconstructed, showing the large shear planes.

### 3.2. Large tension fissures

In the upper third part of the excavation, large tension fissures were observed (Fig. 11).

The planes are irregular and seem to consist of several tension fissures which all grew towards each other. The two large planes observed are dipping towards the north. The spacing seems to be the same as the spacing between the large shear planes, i.e. less than 1 m. The different nuclei are visible. The strike of the surfaces is EW on an average. Dip angles are low ( $20\text{--}30^\circ$ ). All fissures are dipping towards the north. Dip decreases towards the roof.

Like the shear planes, these fissures show aperture up to 3 cm. Oxidation occurred till 2 m of depth (Fig. 12).



Fig. 7. Pictures of the large shear planes. One can see the safety anchors sticking out of the clay (the anchors are pointing towards the Starting Chamber). The surfaces contain clear striations.

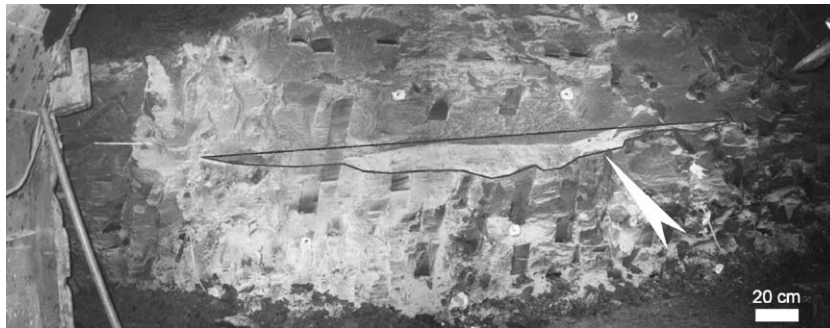


Fig. 8. Picture showing clearly the bowed cross-section of the fractures and the front, indicating that the shear planes are not straight planes, but are more or less circular around the axis of the second shaft.

In Fig. 10, the large tension fissures are also indicated in the cross-section.

#### 4. Comparison of all results: discussion

Looking back on the observations, oxidation was reported to have taken place till a depth of 2 m into the clay mass. Combining this with the observation of the mould of resin, it can be concluded that the fractures must have been open until this depth.

From the observations during the excavation of the Mounting Chamber, it can be concluded that the extent of the EDZ around the second shaft (radius

~ 4.5 m) ranges up to approximately 12 m from the axis of the second shaft into the clay (this is about 6 m behind the wall of the Starting Chamber, see Fig. 3).

In Fig. 13, the results from the BGR campaign are compared with the observations made in the Mounting Chamber. The area, where a strong attenuation of P-waves was observed up to 2 m of depth, might be explained by the open fractures in the clay mass. The high velocity variations between 8.5 and 13.5 seem to be caused by borehole breakouts and the intense fracturing around the borehole.

As a conclusion, it can be stated that the results from the seismic campaign largely correspond with the observations made. Seismic measurements can be useful for the characterisation of the EDZ, especially of the open fractures. Disadvantages of the method are, however, the limited spatial precision of these measurements and the fact that damage of the borehole due to the drilling process disturbs of the measurements. The detection of closed fractures is uncertain, as the increase in P-wave velocity in the first meters of the cross-hole measurements might also be explained by increasing stresses with distance.

Cored borings are very useful for characterisation purposes, although, fractures created during the drilling process again need to be filtered out.

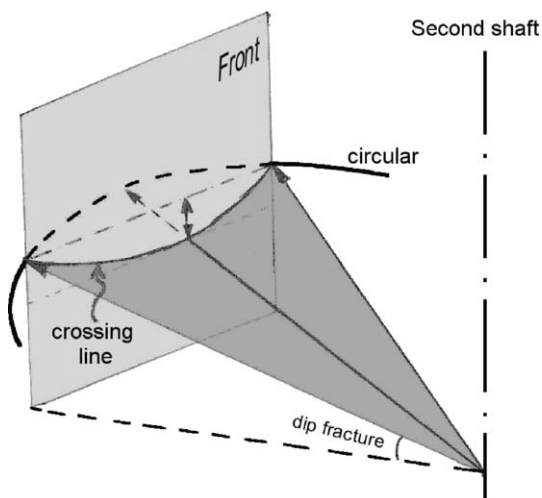


Fig. 9. Drawing explaining the bowed cross-section of the fractures and the front.

#### 5. Origin of the fractures

##### 5.1. Large shear planes

The large slip planes seem to be caused by the excavation of the second shaft and the Starting

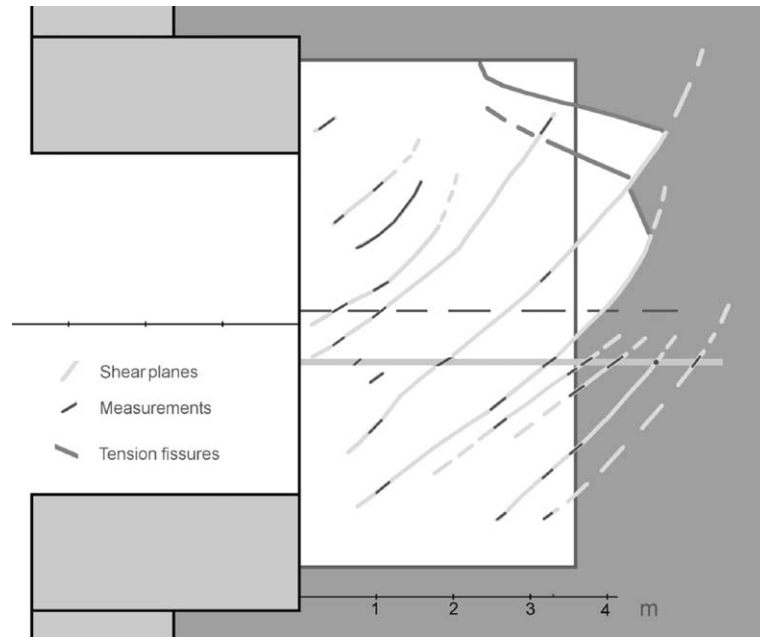


Fig. 10. Vertical cross-section through the Starting and Mounting Chamber. Large fractures (shear planes and tension fissures) are indicated. One can notice that the dip angle of many of the shear planes increases with increasing distance from the second shaft.

Chambers. This is proved by the shape of the rock fall in the Starting Chamber, by observations in the Mounting Chambers, by the strikes of the slip planes encountered in the cores of both drillings (2000–11 and 2001–2), by the form of the cross-section of the planes in the first 2 m of the excavation and by the

average striation orientation. The average strike is also perpendicular to the tunnel axis (which is N–S oriented).

Another argument for this theory is the fact that many of the planes become steeper further away from the second shaft (see Fig. 10).

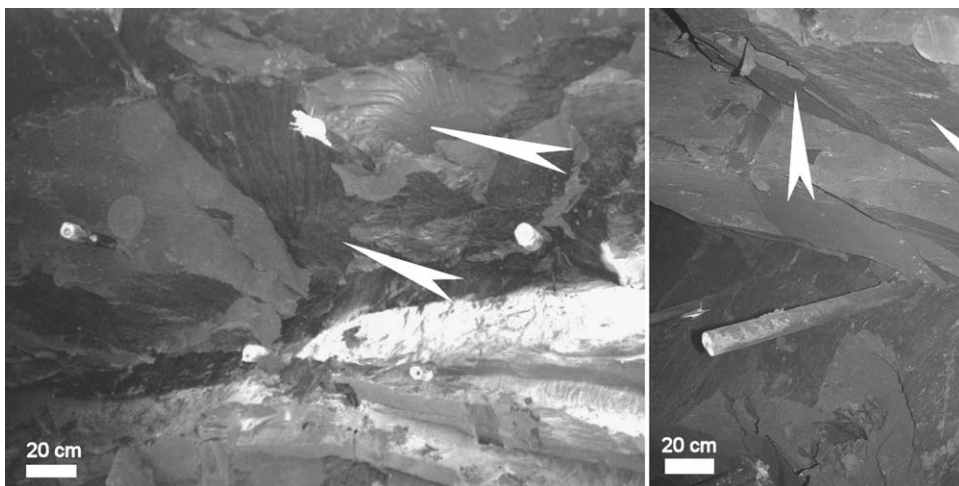


Fig. 11. Picture of large tension fissures. The left picture shows that the fissures consist of several smaller tension fissures which all grew towards each other.



Fig. 12. Oxidation at a depth of 2 m behind the Starting Chamber. The oxidation marks are formed around small pyrite nodules present in the clay.

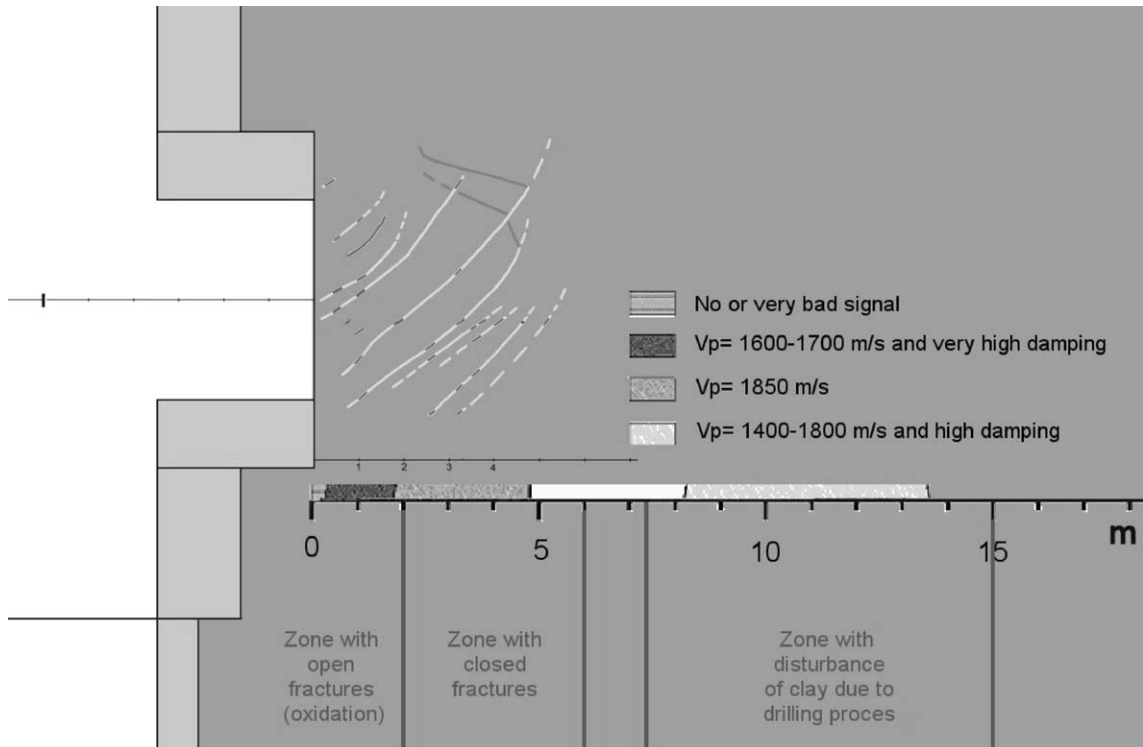


Fig. 13. Comparison of all results from the Mounting Chamber. The reconnaissance campaign is compared to the fractures observed during the excavation of the Mounting Chamber.

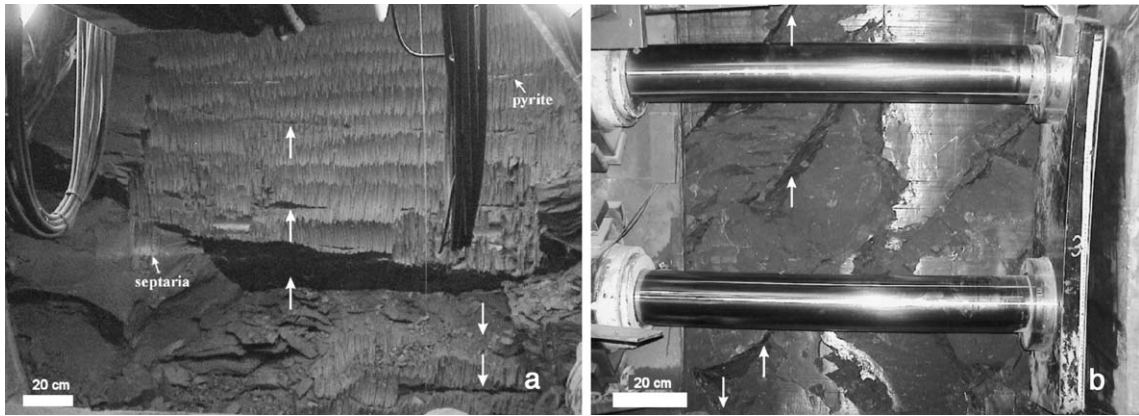


Fig. 14. Pictures of the fracturing in the Connecting Gallery. (a) shows the front. One can see the cross-section of the parallel shear planes, and the intersection is more or less where the block has fallen out. (b) shows a sidewall. The cross-sections of the fractures with the gallery walls were mapped carefully.

Not all planes were regular, especially not near the end of the excavation works (splitting, undulating). The average strike of the planes is, however, still perpendicular to the tunnel axis and no indication was found that any of the large slip planes has a natural origin (this means it was present before excavation of the second shaft).

The planes encountered further away from the second shaft might be caused by the excavation of the second shaft as well as by the excavation of the Starting Chamber. The opening of the fractures in the first 2 m might be caused by a combination of decompression and desiccation.

### 5.2. Large tension fissures

The large tension fissures appeared in the upper third part of the Mounting Chamber (Fig. 10). The strike of the surfaces is on an average perpendicular to

the tunnel axis. They are interpreted as the result of the decompression/gravitational forces, due to the excavation of the Starting Chamber.

## 6. Excavation connecting gallery

The Connecting Gallery (~ 84 m length) was constructed using an industrial excavation technique. A road header under the protection of a steel shield milled off the front. The excavated diameter was 4.89 m and the internal diameter of the lined gallery was 4 m. The shield was equipped with a cutting head to ensure a smooth excavation profile when the shield is pushed forward. Throughout the entire Connecting Gallery project, limiting the convergence of the host rock has been one of the main priorities: the less convergence one allows, the smaller the extent of the EDZ will be. Therefore, the shield is

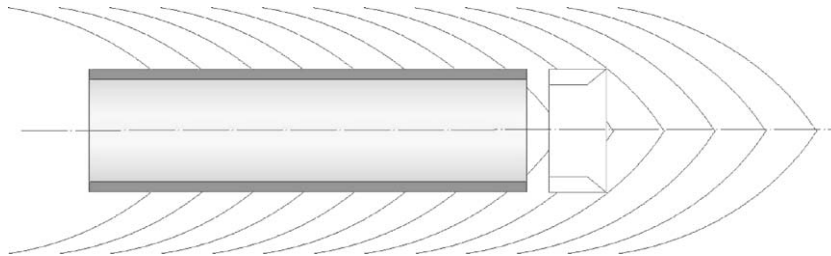


Fig. 15. Schematic representation of a vertical cross-section through the Connecting Gallery showing the typical symmetrical form of the encountered shear planes.

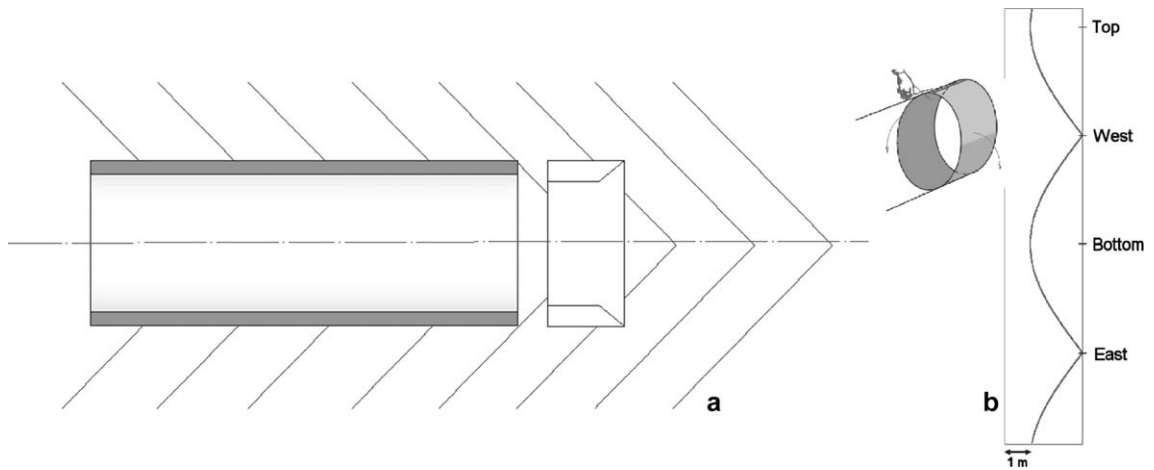


Fig. 16. Analytical calculations of the cross-section of a plane dipping  $50^{\circ}\text{N}$  and  $50^{\circ}\text{S}$  with a cylinder. (a) Simplified fracture pattern. (b) Intersection trace.

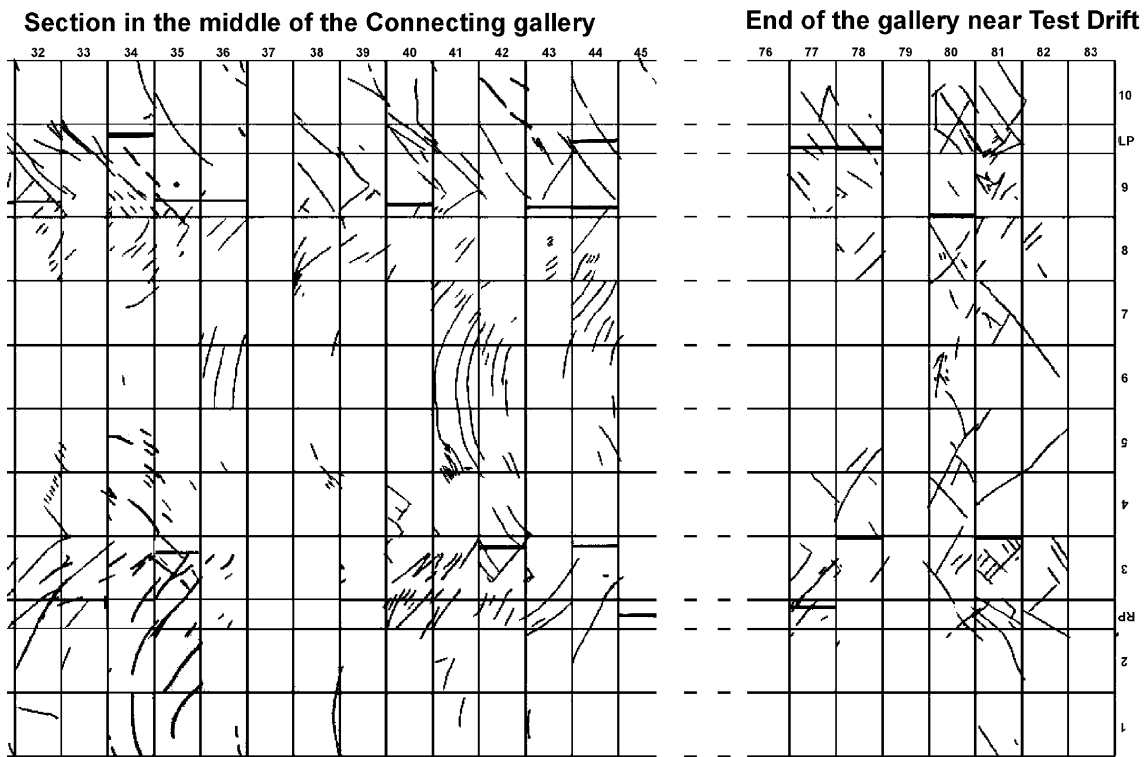


Fig. 17. Unfolded cylinder showing the fracture traces along the walls of the Connecting Gallery. Only two parts are shown here. The left part is representative for the whole gallery, except for the end of it, near the Test Drift. That part is shown on the right side of the figure. One section represents 1 m.

very short (2.3 m) and the lining is placed as soon as possible after excavation. To avoid additional convergence, an expanded lining type (non-reinforced concrete segments) is used: the wedge-block system. For more information, see Bastiaens and Demarche (2003).

The excavation of the Connecting Gallery was accompanied by an extensive instrumentation and observation program. A variety of parameters were registered and studied: excavated diameter, advancement rate, convergence, strains, pore water pressure, displacements, etc. Geological features such as fractures and stratigraphy were also studied. Here, we will focus on the observation and interpretation of the fracturing.

As the excavation progressed, the face and sidewalls of the gallery were observed, mapped and photographed; fractures were characterised by measuring their dip and dip direction when this was possible in safe circumstances. The result is a detailed database describing fracture type and orientation over the whole tunnel length. This information allowed us to determine whether and how the excavation process induced fractures or whether they were naturally induced (pre-existing).

### 6.1. Observations

As mentioned before, the front and sidewalls were systematically observed and the encountered fracture planes were characterised and mapped (Fig. 14).

The orientation of the encountered fractures is consistent along most of the excavation (only in the few first and last meters other types occurred). In the first few meters, the continuation of the fracture planes encountered during the construction of the Mounting Chamber (see Section 3) was observed: large planes, dipping south (towards the second shaft) with an approximately E–W trend. Near the end of the Connecting Gallery, close to the old front of the Test-Drift, fractures that were induced by the excavation of the Test-Drift 15 years ago were observed.

Shortly after the start of the excavation, fracture orientations appeared, other than the ones previously observed during the construction of the second shaft, Starting Chamber and the Mounting Chamber, and a consistent fracture pattern could be recognized. This pattern consists of two conjugated fracture planes: one

in the upper part, dipping towards the excavation direction (north) and one in the lower part, dipping in the opposite direction (south). The two fracture planes intersected at half the height of the gallery; at this point, their dip is up to 60–70° (N or S) but further away from the axis, in a vertical plane (higher or lower), the dip decreases (values as low as 30° have been measured): the planes are curved. The fracture planes are also curved in the other dimension (horizontal plane): the dip direction is parallel to the gallery axis (~ N–S) near the centre of the face but changes towards the east and west sidewalls. The observed

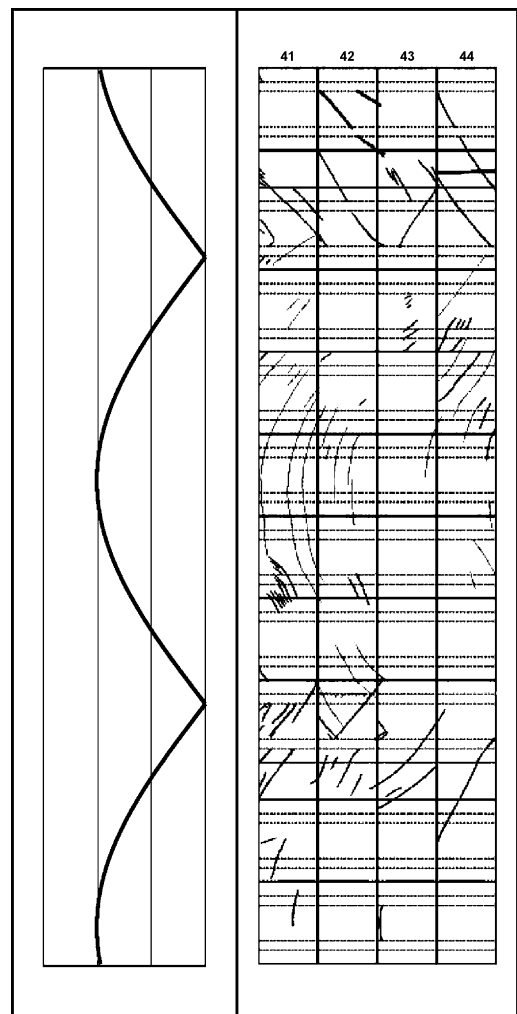


Fig. 18. Comparison between the calculated trace and observed traces along the walls of the Connecting Gallery.

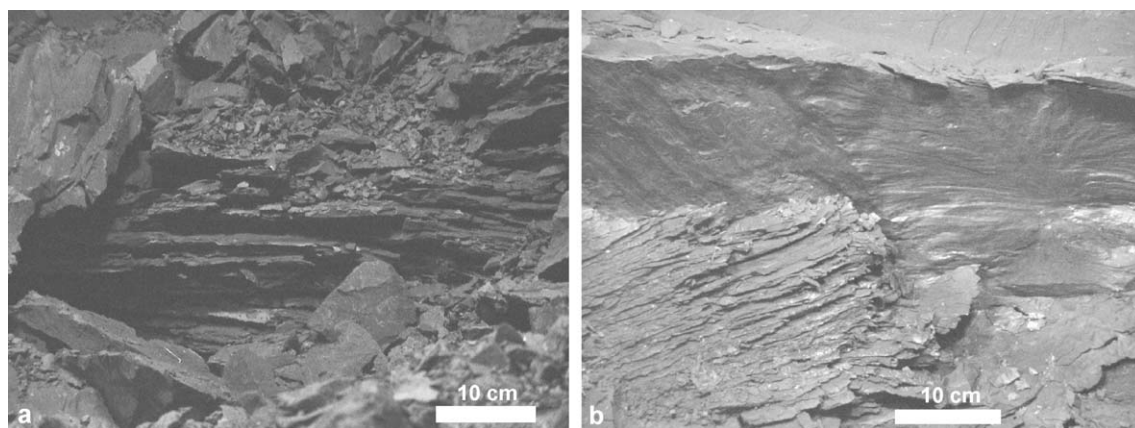


Fig. 19. (a) Fissures due to decompression of the clay. (b) Tension fissures, due to the detachment of clay blocks.

curved shape is schematically drawn on a vertical cross-section in Fig. 15. The distance between subsequent fractures is mostly a few decimeters (Fig. 14).

If the fracture pattern is simplified to two flat fracture planes (one dipping  $50^\circ\text{N}$ , the other  $50^\circ\text{S}$ ) with a trend perpendicular to the gallery axis, the theoretical trace on the gallery sidewalls in the unsupported zone can be calculated as the intersection of the two planes with a cylinder (Fig. 16a). The calculated trace can be found in Fig. 16b: it shows an unfolded cylinder and one band corresponding to 1 m.

Fig. 17 shows the fracture map of the gallery sidewall; the traces of the fractures are again drawn on an unfolded cylinder (gallery). The width of one wedge-block lining ring is 1 m and as a reference, these lining rings are also indicated on the map.<sup>1</sup> The shape of the traces corresponds with the calculated one (Fig. 18).

Near the connection with the Test-Drift, fractures due to the excavation of the Test-Drift 15 years ago were encountered. Their orientation was consistent with that of the fractures induced by the Connecting Gallery: two fracture planes, dipping towards the south in the upper part and towards the north in the lower part (see Fig. 17).

It is important to mention that only shear fracture planes are drawn on this fracture map. These can be recognized by their shiny surface; slickensides are

present (see Fig. 7). Other features were encountered as well but they were not systematically studied. For instance, in the lower part of the front, horizontal decompression fissures were observed (Fig. 19a) and large vertical tension fissures were also seen on the face, as a consequence of the detachment of large blocks (Fig. 19b).

Shortly after the execution of the Connecting Gallery, two cored borings (one eastwards and one downwards) were performed ( $\sim 2.9$  m depth). As observed in the cored boreholes 2000–11 and 2001–2, a lot of fracturation induced by the drilling process was encountered. In the downward cored borehole, fractures probably induced by the excavation of the Connecting Gallery were identified up to 60 cm. In the cores of the eastward boring, fractures probably induced by the excavation of the Connecting Gallery were identified up to 1 m. The average strike of these fractures was  $200^\circ$ , which corresponds with the observed fracture shape.

## 6.2. Discussion

Fig. 20 maps the result of a simplified 2D axisymmetrical Cam clay model, showing axial, radial and differential stresses along the gallery axis. In this case, the initial stress state was chosen to be isotropic (total initial stresses = 4.6 MPa, initial water pressure = 2.2 MPa) which was a slight simplification as  $K_0$  is expected to be 0.9 (SAFIR II). In addition, the clay itself was chosen to be isotropic. Modelling shows that the stress peak is reached 6 m ahead of the

<sup>1</sup> The connecting gallery lining consists of 83 rings, the first 3.5 are situated inside the former Mounting Chamber.

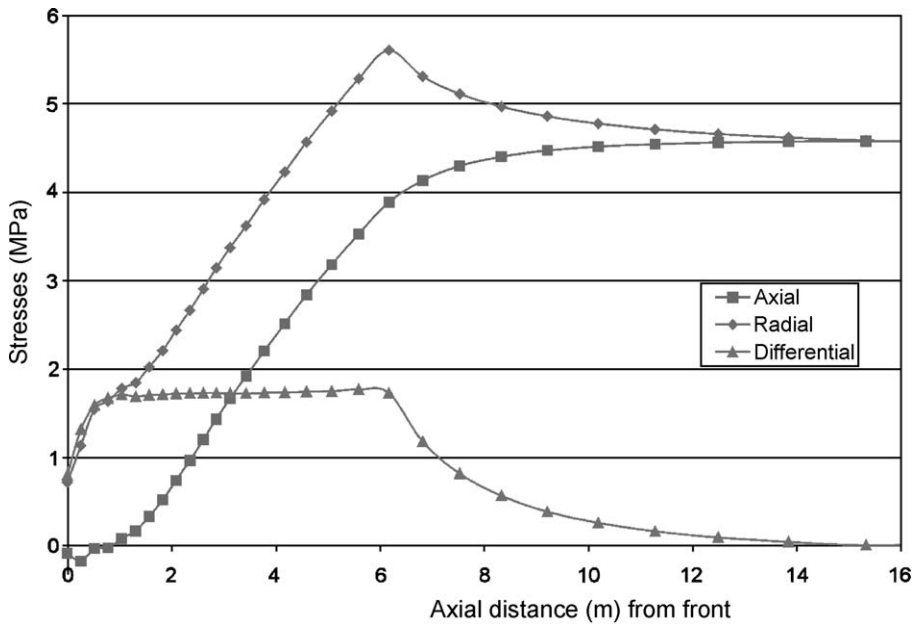


Fig. 20. Modelled stresses (axial, radial and differential) along the gallery axis, ahead of the excavation front (2D axisymmetrical model, using FLAC-code). In this case, the initial stress state was chosen to be isotropic (total initial stresses=4.6 MPa, initial water pressure=2.2 MPa) which was a slight simplification as  $K_0$  is expected to be 0.9 (SAFIR II).

excavation front. It is therefore expected that the fractures are formed several meters ahead of the face.

The shape and orientation of the fracture planes described in the Connecting Gallery is understood

theoretically. It can be explained by the stress redistribution ahead of the gallery face. 2D axisymmetrical Cam clay modelling clearly shows the response of the host rock when a gallery is excavated (Fig. 21)

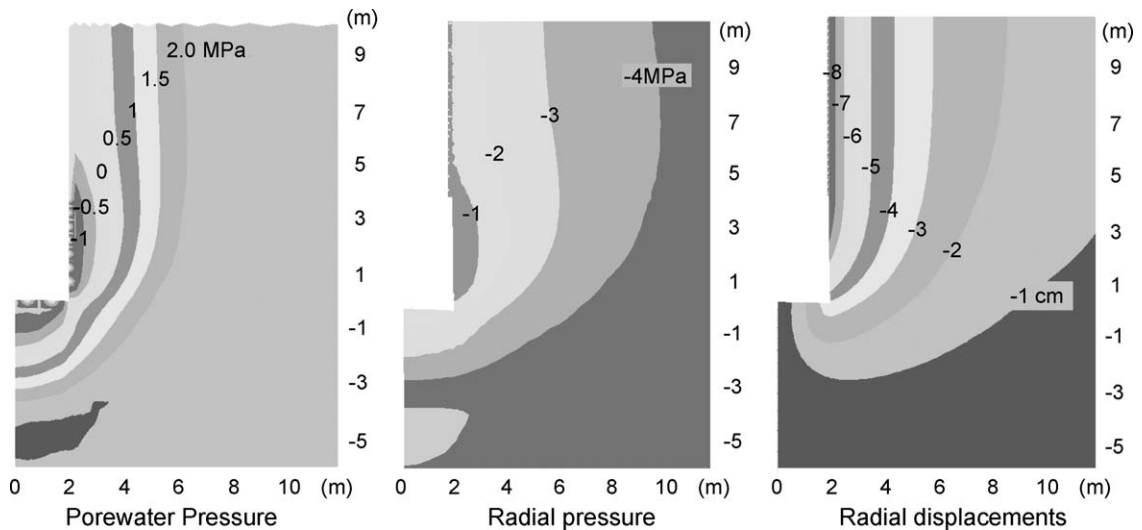


Fig. 21. Modeling results for the spherical response of the host rock when a gallery is excavated (after Bernier and Van Cauteren, 1998). Same boundary conditions as the modeling in Fig. 20 were used.

(Bernier and Van Cauteren, 1998). This corresponds with the curved fracture planes observed in a vertical plane through the Connecting Gallery (Fig. 15). The anisotropy of the fracture pattern, however, needs to be considered. While observations suggest radial isotropy of the fractures in case of the second shaft, this is not the case for the connecting gallery. Possible explanations for this difference in shapes can be the fact that the vertical initial stress is in fact slightly larger than the horizontal one ( $K_0=0.9$ ), or the fact that the clay itself, consisting of compacted clay laminates, is not quite isotropic when comparing a vertical and horizontal section.

It also needs to be remarked that the allowed convergence around the second shaft was significantly higher (order of decimeters) than the convergence allowed around the excavation of the connecting gallery (order of centimeters). It is probably therefore that the ratio of damaged zone to the excavated diameter (EDZ-ratio) is much lower in case of the Connecting Gallery (1.4) than in case of the second shaft (2.7).

The fracture pattern observed in the Connecting Gallery can also be compared with the pattern found in the cored borings at significant distance from the second shaft; these are in fact cylindrical excavations on a small scale (Figs. 5b and 15).

An important issue is that from the description above, it can be concluded that these fractures were induced by the excavation itself. No proof to substantiate the existence of natural induced fractures (pre-existing) in the Boom Clay at the Mol site was found during excavation works.

## 7. Conclusions

The EDZ-ratio around the second shaft could be determined to be 2.7. Fractures are ranging up to 12 m around the axis of this shaft (shaft radius is 4.5 m).

It can be concluded that seismic measurements and cored borings are useful for the characterisation of the Excavation Damaged Zone or EDZ, although disturbance of the borehole (which is comparable with a small-scale excavation) due to the drilling process might influence the results obtained. Velocity increase due to pressure build up also needs to be taken into account. Knowledge about the spatial distribution of the fractures is, however, very limited when using the technique.

Cored borings appeared to be a useful tool to characterise the EDZ, although drilling related fracturing needs to be taken into account.

Excavation works in the Boom Clay at a depth of 223 m always create fracturing, even if convergence is kept to a minimum using industrial techniques. In case of the Connecting gallery, the EDZ-ratio was around 1.4, which is much lower than that of the second shaft.

An explanation for the fracture origin and geometry was presented. It results from a stress redistribution ahead of the face.

So far, no evidence for the occurrence of natural discontinuities was encountered in Mol.

## References

- Bastiaens, W., Demarche, M., 2003. The extension of the URF HADES: realization and observation. Proceedings of the WN'03 Conference, Tucson, USA.
- Bernier, F., Van Cauteren, L., 1998. Instrumentation program near the face of an advancing tunnel in Boom Clay. In: Evangelista, A., Picarelli, L. (Eds.), *The Geotechnics of Hard Soils-Soft Rocks*. Balkema, Rotterdam, pp. 953–959.
- SAFIR II. Safety and Feasibility Interim Report. Nirond 2001-06 E, ONDRAF/NIRAS Brussels.
- Vandenbergh, N., 1978. Sedimentology of the Boom Clay (Rupelian) in Belgium. *Verh. K. Acad. Belg., Klasse aardwetenschappen*, XL (147 pp.).